In vivo tracking of CAR-T cells in tumors via nanobubble-based contrast enhanced ultrasound

Dorian Durig[1], Jude Franklin[1], Reshani Perera[2], Zachary Jackson[3], Hosahalli Vasanna[3], Michael C. Kolios[4], David Wald[3*], Agata A. Exner[1,2*]

Author Address:

[1]Department of Biomedical Engineering, Case Western Reserve University, Cleveland, Ohio 44106, United States

[2]Department of Radiology, Case Western Reserve University, Cleveland, Ohio 44106, United States

[3]Department of Pathology, Case Western Reserve University and University Hospitals Cleveland Medical Center, Cleveland, Ohio 44106, United States

[4]Department of Physics Toronto Metropolitan University, Toronto, Ontario, M5B 2K3, Canada

*To Whom Correspondence Should Be Addressed:

Prof. Agata A. Exner
Department of Radiology, BRB Room 332
Case Western Reserve School of Medicine
10900 Euclid Ave, Cleveland, OH 44145, USA
Agata.exner@case.edu

Or

David N. Wald
Department of Pathology, WRB Room 3-404
Case Western Reserve School of Medicine
2103 Cornell Road, Cleveland, OH 44106, USA
David.wald@case.edu

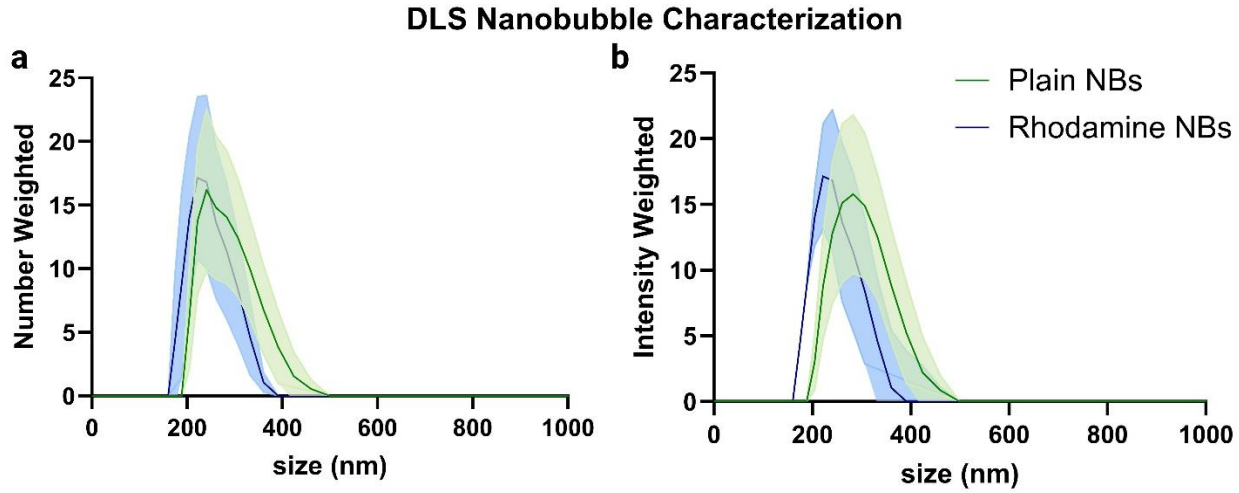

Fig. S1. (a) DLS average number-weighted size distribution of plain C_4F_{10} NBs (no fluorophore), n=3. (b) DLS average intensity-weighted size distribution of rhodamine-labeled C_4F_{10} NBs, n=3. The x-axis is limited to 1000 nm because no particles larger than this size were observed.

Fig. S2. Brightfield microscopy of NBs (scale bar: 5 µm).

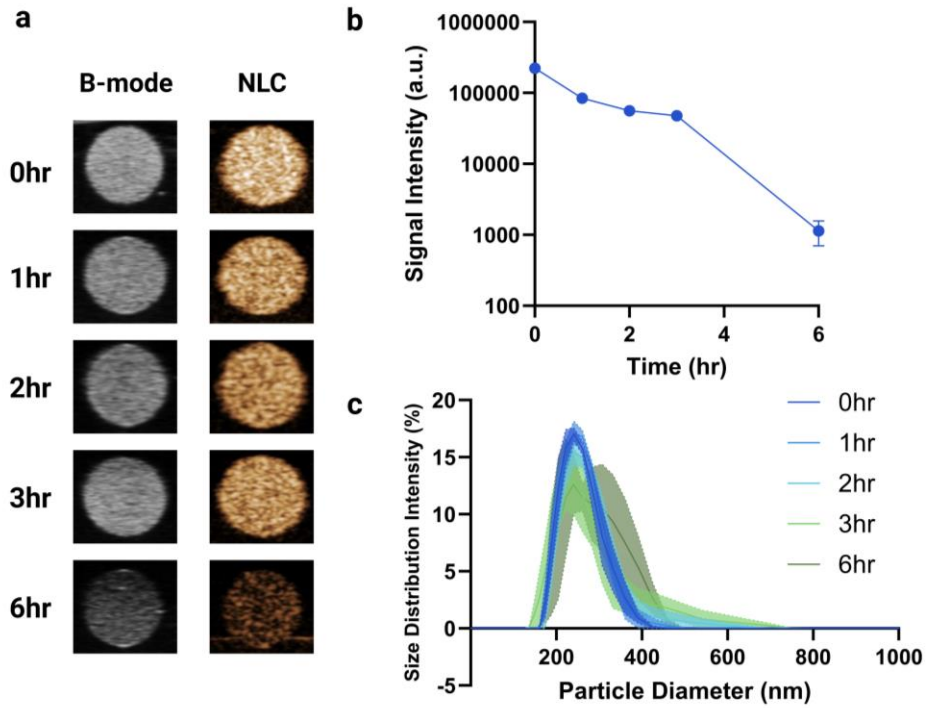

Fig. S3. (a) B-mode and NLC images of NBs incubated in Plasmalyte at 1 x 10^{11} NBs/mL (37 °C, 5% CO_2) and diluted to 1 x 10^8 NBs/mL for Ultrasound imaging at each time point. Dilutions were consistent across samples; however, the reported concentrations correspond to the initial stock and do not account for nanobubble decay during the 0–6 h stability assessment (b) NLC signal intensity over time (n = 3). (c) DLS measurements of NBs diluted to 1 x 10^7 NBs/mL in Plasmalyte over 6 h (n = 3).

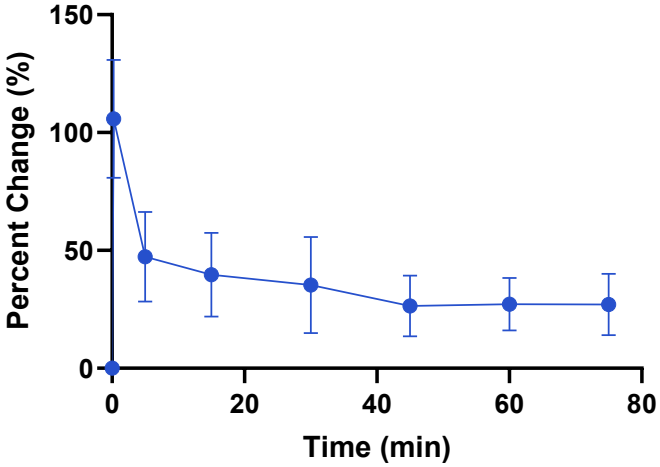

Fig. S4 Percent change in liver NLC signal intensity over time following infusion of NB-labeled CAR-T cells (n = 3), corresponding to the mice used for flow cytometry-based biodistribution analysis of cells in blood and tissues.

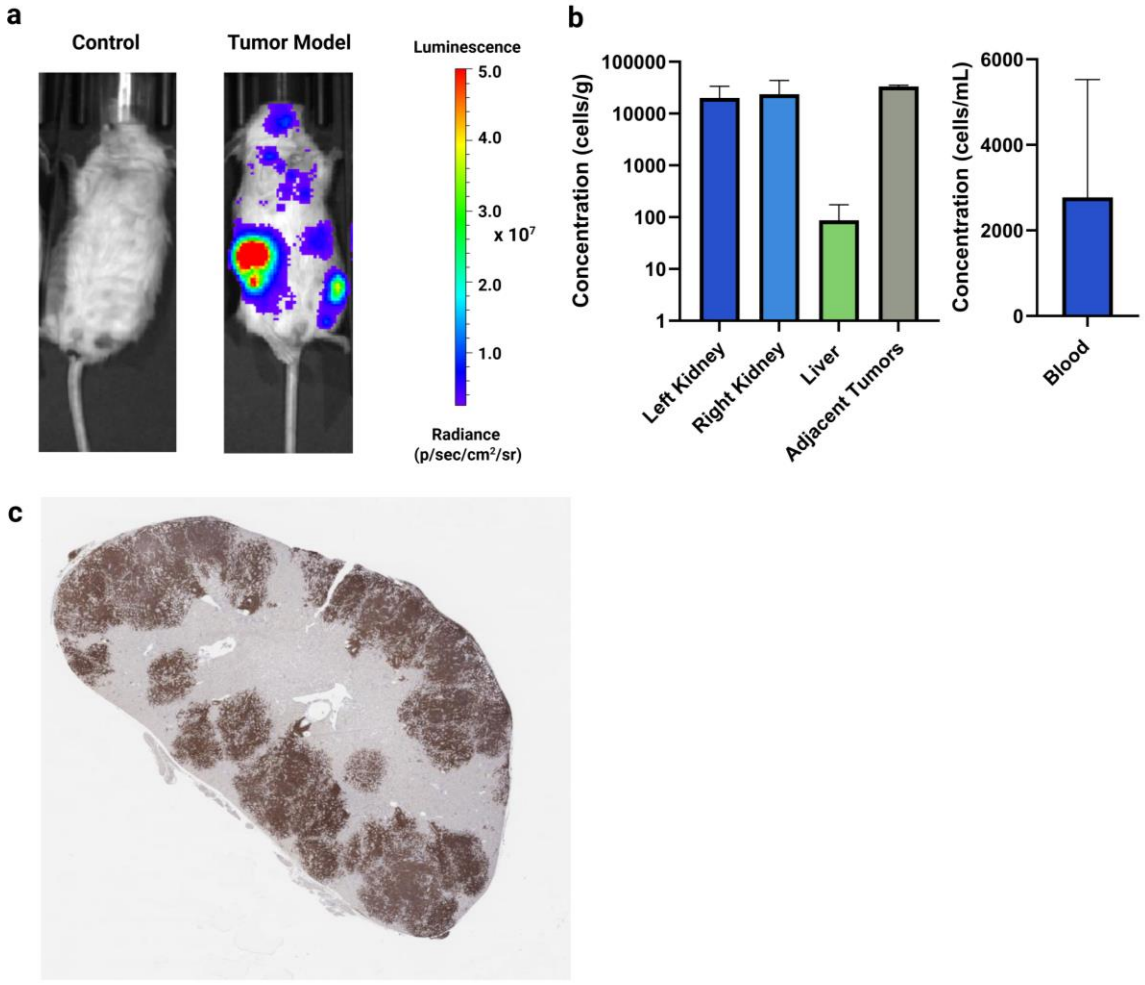

Fig. S5. (a) Representative IVIS bioluminescence images of luciferase-expressing RAJI tumors from control and tumor-bearing mice used in NB-labeled CAR-T cell experiments. (b) RAJI cell concentrations the kidneys, liver, tumor, and blood measured by flow cytometry following NB labeled CAR-T cell injection and US imaging. (c) IHC DAB-stained left kidney from a representative mouse showing CD19-positive RAJI tumor cells to demonstrate tumor burden.

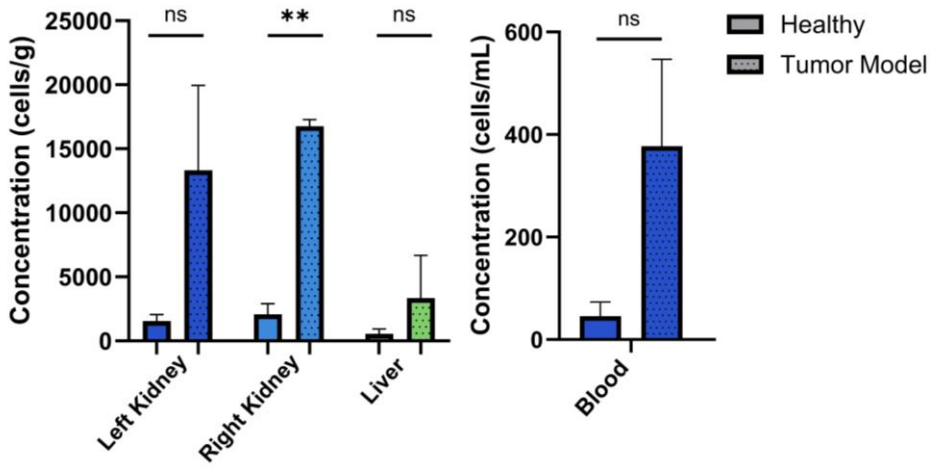

Fig. S6. Flow cytometry CAR-T cell concentrations in liver, kidneys, and blood compared between healthy and tumor-bearing mice after NB-labeled CAR-T cell injection and 75 min imaging. US was performed over the liver (healthy) or left kidney (tumor-bearing).

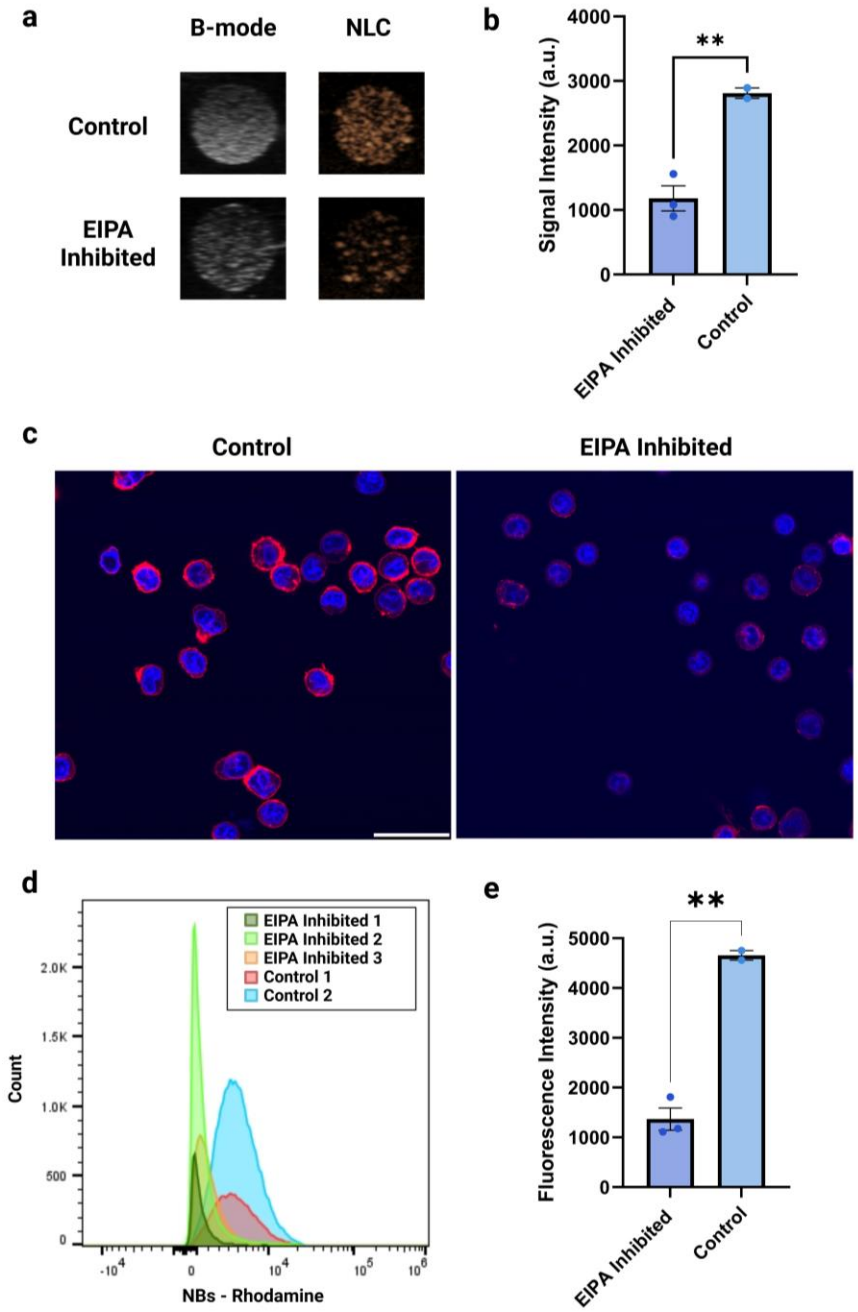

Fig. S7. (a) B-mode and NLC images of rhodamine NB-labeled cells treated with the EIPA inhibitor (n = 3) and untreated control cells (n = 2) . (b) NLC signal intensity of rhodamine NB-labeled cells with EIPA inhibition compared to control. (c) Confocal microscopy images of rhodamine NB-labeled cells (control vs. EIPA-inhibited; scale bar: 25µm); rhodamine gain was maintained between images. (d) Flow cytometry of rhodamine fluorescence from control (n = 2) and EIPA-inhibited (n = 3) CAR-T samples. (e) Median fluorescence intensity per cell, detected by flow cytometry, between EIPA-inhibited and control groups.

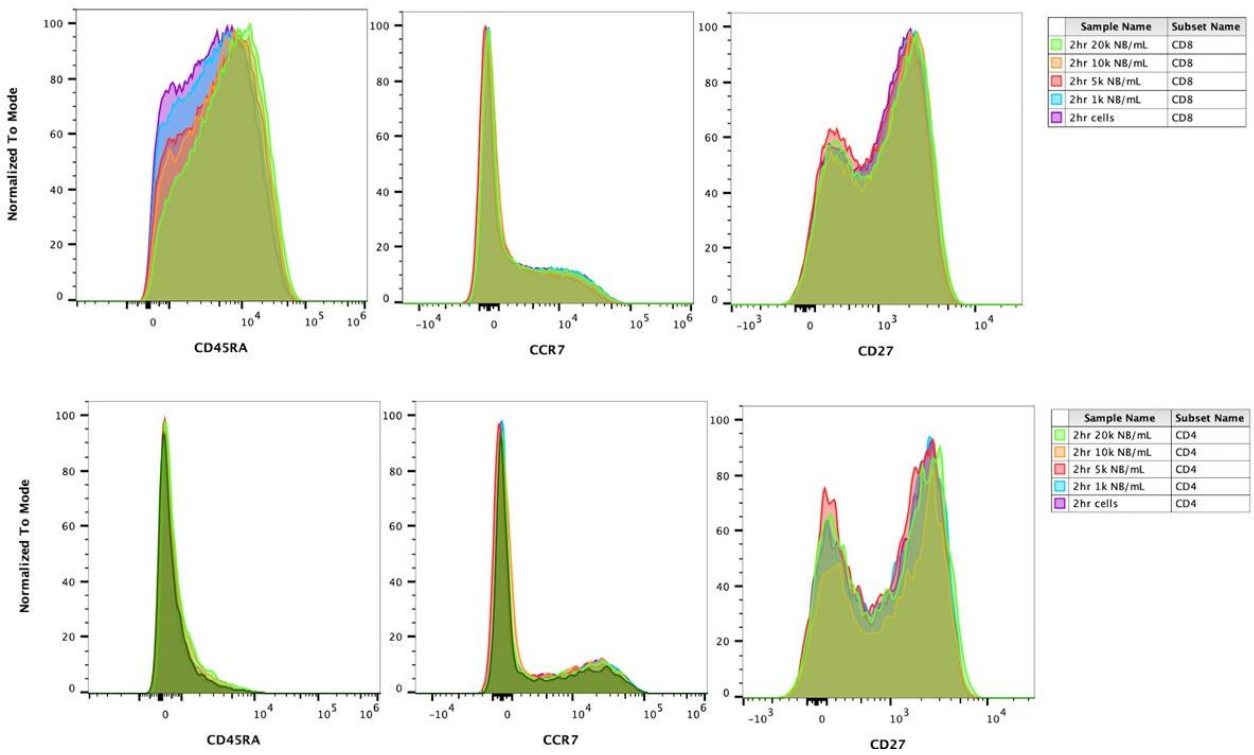

Fig. S8. Flow cytometry analysis of CD8+ and CD4+ T cells stained for CD45Ra, CCR7, and CD27 to assess differentiation phenotypes after a 2-hour incubation with varying concentrations of nanobubbles (0, 1k, 5k, 10k, and 20k NBs/mL). No notable shifts in mean fluorescence intensity (MFI) were observed between subsets, suggesting that nanobubble labeling does not impact T cell differentiation across both CD8+ and CD4+ subsets.